Model for Asymmetry of Shock/Boundary Layer Interactions in Nozzle Flows

Wang Chengpeng[1*], *Zhuo Changfei*[2]

1. College of Aerospace Engineering, Nanjing University of Aeronautics and Astronautics, Nanjing 210016, P. R. China;
2. Department of Aerospace Engineering, Nanjing University of Science and Technology, Nanjing 210094, P. R. China

(Received 11 September 2017; revised 17 November 2017; accepted 27 November 2017)

Abstract: The reason for the asymmetry phenomenon of shock/boundary layer interactions (SBLI) in a completely symmetric nozzle with symmetric flow conditions is still an open question. A model for the asymmetry of nozzle flows was proposed based on the properties of fluid entrainment in the mixing layer and momentum conservation. The asymmetry model is deduced based on the nozzle flow with restricted shock separation, and is still applicable for free shock separation. Flow deflection angle at nozzle exit is deduced from this model. Steady numerical simulations are conducted to model the asymmetry of the SBLIs in a planar convergent-divergent nozzle tested by previous researchers. The obtained values of deflection angle based on the numerical results of forced symmetric nozzle flows can judge the asymmetry of flows in a nozzle at some operations. It shows that the entrainment of shear layer on the separation induced by SBLTs is one of the reasons for the asymmetry in the confined SBLIs.

Key words: asymmetry; shock/boundary layer interactions; nozzle flow; entrainment

CLC number: V211.3 **Document code**: A **Article ID**: 1005-1120(2018)01-0146-08

Nomenclature

A	Area
a	Sonic speed
h	Height of separation bubble
L_1	Length of separation bubble
L_2	Distance between the top of separation bubble and reattachment point
Ma	Mach number, mass
Ma_c	Convective Mach number
$\dot{m}$	Mass flow rate
NPR	Nozzle pressure ratio, p_0/p_a
p	Pressure
r	Velocity ratio across mixing layer
s	Density ratio across mixing layer
T	Time
u	Velocity
V	Volume
α	Nozzle divergence angle
γ	Specific heat ratio
Γ	Index for flow asymmetry
δ_2	Vertical coordinate of the edge of mixing layer on low-velocity side
δ_w	Local thickness of mixing layer
δ'_w	Spreading rate of mixing layer
η	Similarity variable
ρ	Density of fluid
Φ	Normalized spreading rate of mixing layer

Subscripts

0	Stagnation state at nozzle entrance
1	High-velocity side of mixing layer
2	Low-velocity side of mixing layer
a	Ambient condition
b	Separation bubble
e	Entrainment
ex	Nozzle exit
m	Averaged

0 Introduction

Asymmetry phenomenon of shock/boundary layer interaction (SBLI) in a completely symmetric duct with symmetric flow conditions, e. g.,

* Corresponding author, E-mail address: wangcp@nuaa.edu.cn.

How to cite this article: Wang Chengpeng, Zhuo Changfei. Model for asymmetry of shock/boundary layer interactions in nozzle flows[J]. Trans. Nanjing Univ. Aero. Astro., 2018,35(1):146-153.
http://dx.doi.org/10.16356/j.1005-1120.2018.01.0146

an asymmetric shock (see Fig. 1), has been observed frequently by many researchers. The reason for the flow asymmetry is still an open question, and is clarified neither by experiment nor computational fluid dynamics (CFD)[1].

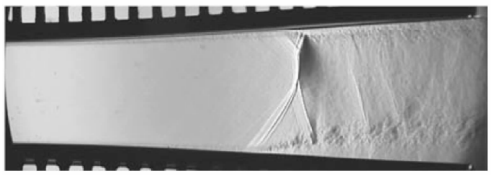

Fig. 1 Experimental schlieren of asymmetric lambda shock in a planar nozzle[2]

When a supersonic nozzle is operated at pressure ratio well below its design point, a shock system forms inside the nozzle and SBLI comes into being, which probably separates flow downstream of the shock from the nozzle walls and brings an asymmetric flowfield. The asymmetry in the nozzle flow can yield dangerous lateral forces, the so-called side-loads, which may damage the nozzle[1]. Lawrence[3] studied the nature of flow asymmetry in planar and axisymmetric nozzles. He observed different symmetric and asymmetric flow structures. Papamoschou et al.[2] experimentally investigated the supersonic nozzle flow separation inside planar convergent-divergent nozzles. Their study shows that for the area ratio of nozzle exit to its throat $A_e/A_t \geqslant 1.4$ and NPR$>$1.4, the flow pattern is asymmetric. This asymmetry does not flip during a given test run, but it can change from one wall to the other and from one run to the next. This phenomenon was also observed by Shimshi et al.[4]. Bourgoing et al.[5] found that shock configuration in a Mach 2 planar nozzle is transformed from a symmetric pattern to an asymmetric one and asymmetric one again with the variation of NPR. A series of large-eddy simulations (LES) were conducted by Olson et al.[6] to model the asymmetry and unsteadiness of the SBLI in the planar nozzles tested by Ref. [2].

Based on the aforementioned research on the asymmetry of SBLI in nozzles, some basic conclusions can be drawn:

(1) Asymmetry of confined SBLI is closely relevant to the strength of SBLI, i.e., the shock intensity and the confinement level.

(2) Asymmetry of SBLI has a flipping phenomenon, i.e., asymmetric shock system can flip between two sides of a nozzle. Flipping does not happen during a given test run in nozzle experiments, but could takes place between runs.

The reason for the asymmetry of confined SBLI is not clear yet, but many researcher, e.g., Lawrence[3], Papamoschou et al.[2], Myshenkov[7], Wang[8], attributed it to Coanda effect which is used for the tendency of a fluid jet issuing tangentially on to a curved or angled solid surface to adhere to it[9]. The entrainment of jet on ambient fluid is regarded as the cause for Coanda effect, but so far it has not been understood completely yet[10], even though it has been applied widely in industry. Coanda effect was confirmed experimentally by Allery et al.[11] to work in symmetrical configurations as it does in the single wall case: the jet reattaches randomly to either of two walls.

The study is motivated by the research of Piponniau et al.[12] who proposed a model based on the properties of fluid entrainment in the mixing layer to explain low frequency unsteadiness on shock induced separation. Due to the close relation between his model and Coanda effect, Piponniau's model is developed further here to explain the reason for the asymmetry of SBLI in an overexpanded nozzle whose flowfield data were obtained by numerical simulations.

1 Theory

1.1 Aerodynamic scheme

According to Piponniau et al.[12], when a separation bubble is produced by SBLI (Fig. 2), in the first part of the bubble, that is from the separation line, eddies are formed in the mixing layer zone (the reversed flow in the separation bubble is regarded as the other stream) and grow as it moves downstream. Fluid from the separated zone is entrained by the mixing layer. Near the middle of bubble (where the mixing layer has

the maximum thickness), these eddies are shed into the downstream flow, bringing with them their mass, momentum and vortices outside the separated region. This generates, in the recirculating region, a default of mass that increases over time. Therefore, when the flow reattaches downstream, the mass amount inside the bubble decreases.

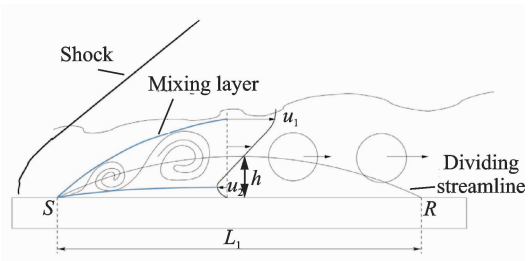

Fig. 2 Sketch of the entrainment of mixing layer on separation bubble[12]

Now we consider the situation of asymmetric SBLI in a 2D nozzle, whose flowfield pattern is sketched in Fig. 3. Coanda effect works in this flow, entrainment of mixing layer on separation bubble on the upper wall decreases the mass and pressure inside the bubble, and the opposite phenomena happen on the lower wall. The pressure difference between two sides deflects the flow behind the shock to the upper wall. To understand how the result of asymmetry takes place, an imaginary symmetric flowfield, which is supposed to be the situation before the asymmetric flow pattern appearing, is sketched in Fig. 4. Prior to create the asymmetry model, three assumptions are made in this situation:

(1) Based on the feature of Conada effect introduced in Introduction, it is assumed that the entrainment of mixing layer only activates on one side, while the separation bubble on the other side keeps constant.

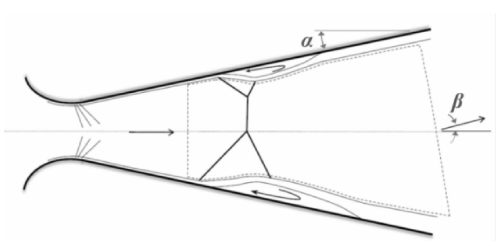

Fig. 3 Asymmetric SBLI pattern in a 2D nozzle

(2) After the shedding of eddies, the mass and pressure decrease inside the bubble but its size keeps constant.

(3) If the final flow is still symmetric, a new amount of reversed flow from downstream enters the bubble at reattachment point R to insure the balance[13].

In the plane reflected shock case, large vortices are shed downstream at the position where the mixing layer reaches its maximum thickness, i. e., the position with maximum separation bubble thickness, which is approximately at the middle of separation bubble[14]. But for SBLI in a nozzle, the situation is a little different, the divergent wall leads to slender rear of separation bubble, and the maximum thickness of the bubble lies in the front of it instead of the middle as the plane case. Therefore, the shedding position for large vortices is still regarded as the position with the maximum bubble thickness in the nozzle case, but not at the middle of bubble. The distance from large vortices shedding position to the reattachment point is denoted as L_2 (Fig. 4).

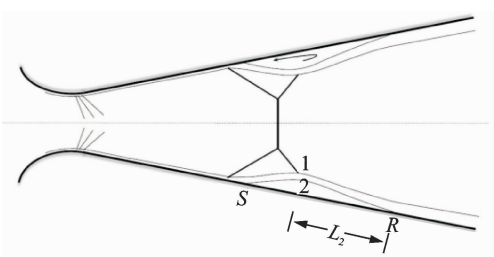

Fig. 4 Imaginary symmetric SBLI flowfield before asymmetric flow taking place in a 2D nozzle

Based on the above assumptions and deduction, now we can discuss the total mass entrained from separation bubble. Total entrained mass is the product of entrainment mass rate $\dot{m}_e$ and entrainment time T_e. The rate of mass entrainment can be obtained from Piponniau's model, which will be deduced later. According to the third assumption, the distance between mass escaping from the bubble and mass returning into the bubble is L_2, and then the time used for entrainment is given by

$$T_e = \frac{L_2}{a_2} \tag{1}$$

where a_2 is the sonic speed on the low-velocity side of the mixing layer.

With the total entrained mass, the pressure inside the bubble after entrainment can be obtained based on the second assumption. Finally, the deflection angle of the flow will be obtained from the longitudinal momentum conservation equation, which will be compared with the actual deflection angle of the flow.

1.2 Theoretical model for flow deflection with entrainment

According to entrainment model of Piponniau's, the separation bubble is approximated by a triangle of length L_1 and height h (Fig. 2), with an average density of ρ_m, then the air mass in the bubble by unit span is given by

$$Ma_b = \frac{1}{2}\rho_m L_1 h \tag{2}$$

And rate of mass entrainment [11]

$$\dot{m}_e = \int_{\delta_2(x_0)}^{y_0(x_0)} \rho u \,\mathrm{d}y = \rho_m \delta_w(x_0) \int_{-\frac{1}{2}}^{0} u \,\mathrm{d}\eta = \rho_m u_1 \delta'_w x_0 \left[(1-r)C + \frac{r}{2}\right] \tag{3}$$

where $\delta_2(x)$ is the vertical coordinate of the edge of the mixing layer on the low-velocity side, $y_0(x)$ the vertical coordinate of the centerline of the mixing layer, and $x_0 = L_3 = L_1 - L_2$ the position where large eddies shed, η is the similarity variable, and the constant $C \doteq 0.14$. δ_w and δ'_w are the local thickness and the spreading rate of the mixing layer, respectively, and the latter can be expressed by the following relation according to Ref. [15]

$$\delta'_w = \frac{\delta'_{ref}}{2}\frac{(1-r)(1+\sqrt{s})}{1+r\sqrt{s}}\Phi(Ma_c) \tag{4}$$

where $\delta'_{ref} \doteq 0.16$ is the spreading rate for subsonic half jet[16]. $r = u_2/u_1$ and $s = \rho_2/\rho_1$ are the velocity ratio and density ratio across the mixing layer, respectively. The function $\Phi(Ma_c)$ is the normalized spreading rate of mixing layer and is dependent on the convective Mach number Ma_c

$$Ma_c = \frac{u_1 - u_2}{a_1 + a_2} \tag{5}$$

$\Phi(Ma_c)$ must be determined via experiment[17] and Fig. 5 gives its empirical value depending on the convective Mach number. Piponniau et al. [12] introduced a function g as

$$g(r,s) = \frac{\delta'_{ref}}{2}\frac{(1-r)(1+\sqrt{s})}{1+r\sqrt{s}}\left[(1-r)C + \frac{r}{2}\right] \tag{6}$$

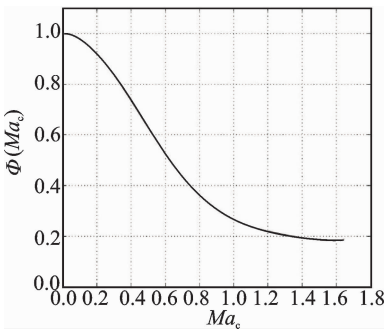

Fig. 5 Normalized spreading rate as a function of the convective Mach number [12]

Finally, the rate of mass entrainment is obtained.

$$\dot{m}_e = \rho_m L_3 u_1 \Phi(Ma_c) g(r,s) \tag{7}$$

Consequently, we discuss the pressure variation in the bubble. The total mass of entrainment

$$Ma_e = \dot{m}_e T = \rho_m L_3 L_2 \frac{u_1}{a_2}\Phi(Ma_c) g(r,s) \tag{8}$$

Based on the second assumption, the volume of bubble keeps constant, and the temperature in the bubble can be considered as invariant, then the density and pressure in the bubble after entrainment

$$\rho_e = \frac{Ma_b - Ma_e}{V_b} = \rho_m\left[1 - \frac{2L_3}{L_1}\frac{L_2}{h}\frac{u_1}{a_2}\Phi(Ma_c)g(r,s)\right] \tag{9}$$

$$p_e = \frac{\rho_e}{\rho_m} p_m = p_m\left[1 - \frac{2L_3}{L_1}\frac{L_2}{h}\frac{u_1}{a_2}\Phi(Ma_c)g(r,s)\right] \tag{10}$$

where p_m is the average pressure in the bubble. Then according to the first assumption, the pressure difference between two sides in the nozzle is obtained.

$$\Delta p = \frac{2L_3}{L_1}\frac{L_2}{h}\frac{u_1}{a_2} p_m \Phi(Ma_c) g(r,s) \tag{11}$$

Eq. (11) can also be written as

$$\Delta p = \frac{2L_3}{L_1}\frac{L_2}{h}\sqrt{\frac{T_1}{T_2}}\, Ma_1 p_m \Phi(Ma_c) g(r,s) \tag{12}$$

With the pressure difference obtained from the above, we can calculate the deflection angle of flow, concerning the vertical momentum conservation for the control volume in Fig. 4.

$$\Delta p\, L_1 \cos\alpha - p_{ex}\, h_{ex} \sin\beta = \dot{m}\, u_e \sin\beta \quad (13)$$

where L_1 is the length of separation bubble in the imaginary symmetric flow, p_{ex} the pressure at nozzle exit, h_{ex} the mainstream height at nozzle exit, α is the nozzle divergence angle, and β is the deflection angle of flow from horizontal direction on the nozzle symmetry plane (Fig. 3). Then, from Eq. (13) we obtain

$$\beta = a\sin \frac{\Delta p\, L_1 \cos\alpha}{p_{ex}\, h_{ex} (\gamma Ma_{ex}^2 + 1)} \quad (14)$$

The above asymmetry model is deduced based the nozzle flow with closed separation bubble, namely, restricted shock separation (RSS)[1]. When the separation zone is open to the ambiance, namely, free shock separation (FSS) (Fig. 6), although the situation is a little different from RSS, the theoretical model created above is still applicable in this case. Now separation length L_1 is the distance from the onset of separation to the nozzle exit, and L_2 the distance from the position with maximum separation thickness to the nozzle exit.

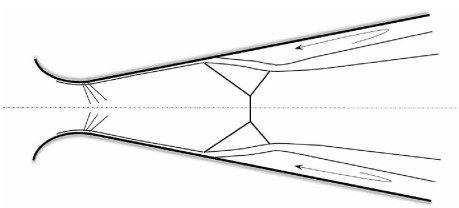

Fig. 6 Imaginary symmetric nozzle SBLI flowfield with FSS

2 Model Application Based on Numerical Results of a Nozzle

2.1 Nozzle geometry and numerical methods

Simulations were conducted to obtain the detailed features of asymmetric SBLI in a planar nozzle. The nozzle model chosen for simulation is a planar nozzle tested by Papamoschou et al.[2] and simulated by Xiao et al.[18], which has a throat height of 22.9 mm, a length of 117 mm and an area ratio (the area ratio of nozzle exit to throat) of 1.5. The nozzle is "trumpet-shaped" with the wall angle increasing monotonically from throat to exit. The maximum nozzle divergence angle is 3.83°.

To apply the asymmetry model proposed above, forced symmetric (half) and full nozzle model were simulated, respectively. The Reynolds-averaged governing equations for compressible turbulent flow with a two equation SST turbulence model in CFX software was employed to simulate idea gas ($\gamma = 1.4$) steady flows. The grid used in the simulations has a higher density near the wall and the minimum first grid point from the wall gives $y^+ < 1$. The total number of grids used is 89 800 for the full model and 51 900 for the half model. Adiabatic, no slip wall boundary condition was specified for all the walls in these simulations.

Computations were made for NPR between 1.20 and 2.40 by changing the total pressure at the nozzle entrance. Other boundary conditions were imposed as follows: The ambient pressure surrounding nozzle exit $p_a = 101\ 325$ Pa, total temperature at nozzle entrance $T_{t0} = 290$ K.

2.2 Numerical results of asymmetric SBLI in full nozzle

Fig. 7 shows the pressure distributions on the two walls of the nozzle from simulations and experiments at two NPRs (the abscissa is normalized by the height of nozzle throat h_t and the vertical axis is normalized by total pressure at nozzle entrance p_{t0}). Note that the nozzle throat is located at $x = 0$. It can be seen that the flow is symmetric at NPR = 1.27 and is asymmetric at NPR = 1.61 based on both numerical and experimental data. At NPR = 1.61, though both numerical and experimental results give the asymmetric flowfield, the deflection direction of flow is opposite: The flow from simulation is deflected downward while that from experiment is deflected upward, which is caused by the randomicity of Coanda effect (entrainment) mentioned in Section 1. The shock positions from simulations are a little more upstream than experimental data, except

this difference numerical results are satisfactory.

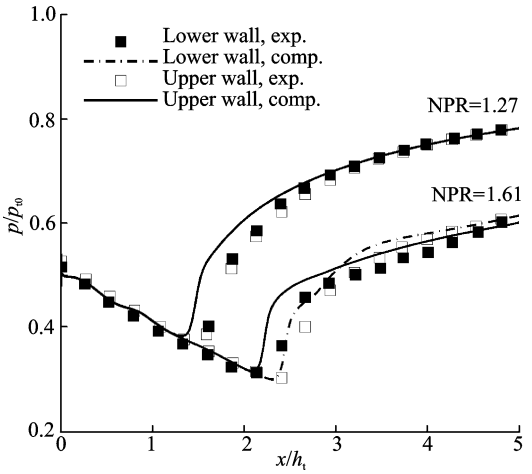

Fig. 7 Wall pressure distributions of the nozzle from simulations and experiments

Three typical flow patterns at different NPRs are shown with numerical schlieren in Fig. 8. At NPR=1.27, a symmetric flowfield with RSS on two sides is presented as Fig. 8(a). At NPR=1.61, an asymmetric flowfield with FSS on one side and RSS on the other side appears as Fig. 8(b). At NPR=2.40, a symmetric flowfield with FSS on two sides is obtained as Fig. 8(c).

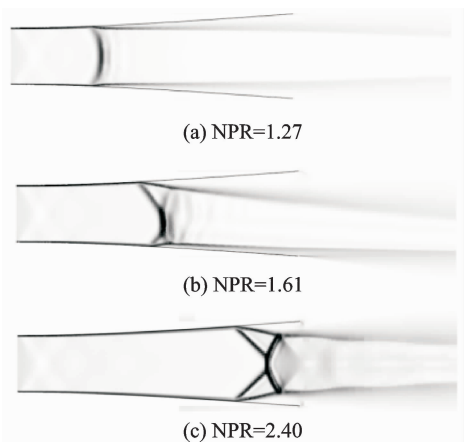

Fig. 8 Typical flow patterns in an over-expanded nozzle with numerical schlieren

Deflection angle of nozzle exit flow at different NPRs are shown in Fig. 9 (squares). It can be seen that the flow in the nozzle is symmetric as Fig. 8 (a) when NPR≤1.27, while it is asymmetric as Fig. 8(b) after that and deflection angle becomes larger and larger with increasing NPR up to 2.10 where the peak asymmetry reaches. Then, the flow returns to be symmetric as Fig. 8(c) when NPR>2.20.

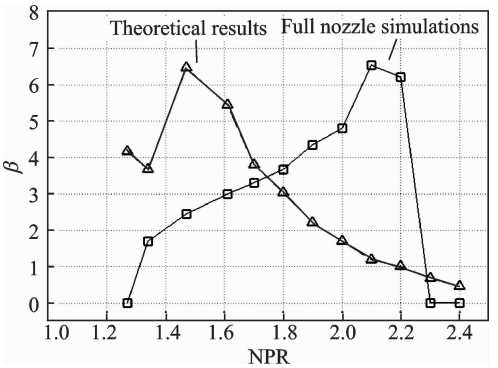

Fig. 9 Deflection angle of flow in the nozzle exit from full nozzle simulations and theoretical results

2.3 Model application based on numerical results of half nozzle with forced symmetry

The nozzle flowfields with forced symmetry were computed to apply the asymmetry model. The numerical results show that the flows with RSS (Fig. 10(a)) were obtained when NPR≤1.61, while the flowfields with FSS (Fig. 10(b)) were attained when NPR≥1.70. According to Eq. (14), the theoretical values of deflection angle of flow at nozzle exit at different NPRs have been calculated, which have been shown in Fig. 9 (triangles). One can see that there is a large difference between the results from theoretical model and actual deflection from full nozzle simulations. Theoretical results give a peak of deflection angle at NPR=1.47 and then decrease gradually, which are close to the deflection offull nozzle only around NPR=1.70 and NPR≥2.30. The results show that there may be other factors to

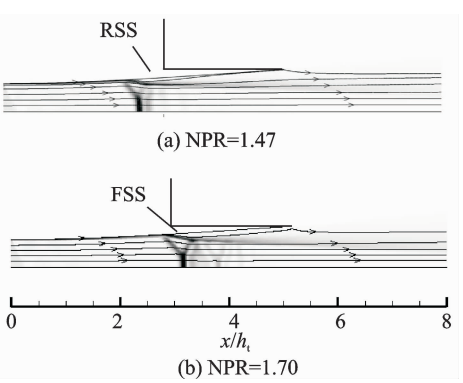

Fig. 10 Numerical schlieren and streamlines of nozzle flow with forced symmetry

control the flow asymmetry besides Coanda effect. Table 1 gives the aerodynamic parameters of the separation at typical NPRs.

Fig. 11 gives averaged pressure in the larger separation of full nozzle and in the separation of half nozzle with force symmetry, which shows averaged pressure in the separation on the side without entrainment is nearly constant before and after flow deflection at most NPRs except NPR=1.34, and consequently proves the validity of the first assumption in Section 1.1.

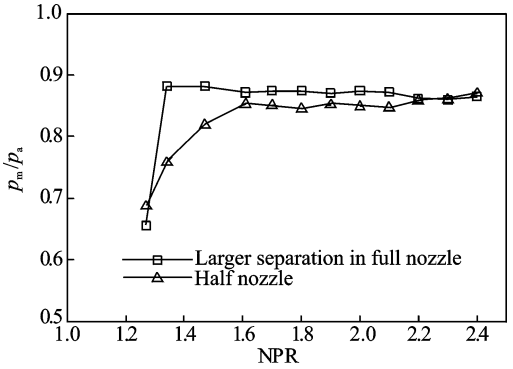

Fig. 11 Averaged pressure in the separation

Table 1 Aerodynamic parameters of separation at typical NPRs for half nozzle with forced symmetry

NPR	T_1/T_2	Ma_1	r	s	$g(r,s)/10^{-2}$	Ma_c	$\Phi(Ma_c)$	h/mm	L_1/m	L_2/mm	p_2/p_{ex}	Ma_{ex}	h_{ex}/mm
1.27	0.86	0.93	−0.033	0.84	2.09	0.46	0.67	0.15	11.4	6.8	0.69	0.53	34.35
1.47	0.84	1.01	−0.107	0.81	1.89	0.54	0.58	1.2	49.6	39	0.71	0.67	34.35
1.61	0.81	1.06	−0.128	0.79	1.80	0.57	0.55	1.7	58.0	46	0.74	0.76	30.95
2.2	0.80	1.16	−0.160	0.73	1.64	0.63	0.49	3.2	32.9	15	0.76	1.15	27.95
2.3	0.79	1.21	−0.157	0.80	1.70	0.66	0.47	3.4	29.7	11	0.77	1.15	27.55
2.4	0.76	1.26	−0.161	0.78	1.67	0.68	0.46	3.5	27.0	7	0.79	1.15	27.35

3 Conclusions

A model for the asymmetry of SBLI in nozzle flows has been proposed based on the properties of fluid entrainment in the mixing layer and momentum conservation. Deflection angles obtained from the theoretical model based on the simulation results of a half nozzle with forced symmetry show a large difference from those of the actual full nozzle, which shows there should be other factors to control the flow asymmetry besides Coanda effect (or entrainment), and the entrainment of shear layer on the separation induced by SBLI is just one of causes for the asymmetry.

Acknowledgements

This work was supported by the National Natural Science Foundations of China (Nos. 51476076, 51776096).

References:

[1] HADJADJ A, ONOFRI M. Nozzle flow separation [J]. Shock Waves, 2009, 19(4): 163-169.

[2] PAPAMOSCHOU D, ZILL A, JOHNSON A. Supersonic flow separation in planar nozzles[J]. Shock Waves, 2009, 19(3): 171-183.

[3] LAWRENCE R A. Symmetrical and unsymmetrical flow separation in supersonic nozzles: Research Report Number 67-1[R]. [S. l.]: Southern Methodist University, 1967.

[4] SHIMSHI E, BEN-DOR G, LEVY A, et al. Experimental investigation of asymmetric and unsteady flow separation in high Mach number planar nozzles [C]// Proceedings of the 28 th International Symposium on Shock Waves. Manchester: [s. n.], 2011.

[5] BOURGOING A, REIJASSE P. Experimental analysis of unsteady separated flows in a supersonic planar nozzle[J]. Shock Waves, 2005, 14(4): 251-258.

[6] OLSON B J, LELE S K. A mechanism for unsteady separation in over-expanded nozzle flow[J]. Physics of Fluids, 2013, 25:110809.

[7] MYSHENKOV E V. Hysteresis phenomena in a plane rotatable nozzle[J]. Fluid Mechanics, 2010, 45(4): 667-678.

[8] WANG T S. Transient two-dimensional analysis of side load in liquid rocket engine nozzles: AIAA 2004-3680[R]. USA: AIAA, 2004.

[9] NEUENDORF R, WYGNANSKI I. On a turbulent wall jet flowing over a circular cylinder[J]. J Fluid Mech, 1999, 381: 1-25.

[10] MIOZZI M, FRANCESCO L, ROMANO G P. Experimental investigation of a free-surface turbulent jet with Coanda effect[C]// 15th Int Symp on Applications of Laser Techniques to Fluid Mechanics. Lisbon, Portugal:[s. n.],2010.

[11] ALLERY C, GUERIN S, HAMDOUNI A, et al. Experimental and numerical POD study of the Coanda effect used to reduce self-sustained tones[J]. Mechanics Research Communications, 2004, 31: 105-120.

[12] PIPONNIAU S, DUSSAUGE J P, DEBIEVE J F, et al. A simple model for low-frequency unsteadiness in shock induced separation[J]. J Fluid Mech, 2009, 629: 87-108.

[13] SIMPSON R L. Turbulent boundary-layer separation [J]. Annu Rev Fluid Mech, 1989, 21: 205-234.

[14] DUPONT P, HADDAD C, DEBIEVE J F. Space and time organization in a shock induced boundary layer [J]. J Fluid Mech, 2006, 559: 255-277.

[15] PAPAMOSCHOU D, ROSHKO A. The compressible turbulent shear layer: An experimental study[J]. J Fluid Mech, 1988, 197: 453-477.

[16] BROWAND F K, TROUTT T R. The turbulent mixing layer: Geometry of large vortices[J]. J Fluid Mech, 1985, 158: 489-509.

[17] SMITS A J, DUSSAUGE J P. Turbulent shear layers in supersonic Flow[M]. New York: AIP Press, 2006: 155-156.

[18] XIAO Q, TSAI H M, PAPAMOSCHOU D. Numerical investigation of supersonic nozzle flow separation[J]. AIAA J, 2007, 45(3): 532-541.

Dr. **Wang Chengpeng** is currently an associate professor in College of Aerospace Engineering, Nanjing University of Aeronautics and Astronautics (NUAA). He received his Ph. D. degree in NUAA. His research interests are high speed aerodynamics, experimental aerodynamics.

Dr. **Zhuo Changfei** is currently a lecturer in Department of Aerospace Engineering, Nanjing University of Science and Technology. He received his Ph. D. degree in NUST. His research interests are high speed aerodynamics.

(Production Editor: Zhang Tong)